

Product-state distributions in the dissociative recombination of ${}^3\text{HeD}^+$ and ${}^4\text{HeH}^+$

J. Semaniak,¹ S. Rosén,¹ G. Sundström,¹ C. Strömholm,¹ S. Datz,² H. Danared,³ M. af Ugglas,³ M. Larsson,¹ W. J. van der Zande,⁴ Z. Amitay,⁶ U. Hechtischer,⁵ M. Grieser,⁵ R. Repnow,⁵ M. Schmidt,⁵ D. Schwalm,⁵ R. Wester,⁵ A. Wolf,⁵ and D. Zajfman⁶

¹Department of Physics I, Royal Institute of Technology (KTH), S-100 44 Stockholm, Sweden

²Physics Division, Oak Ridge National Laboratory, Oak Ridge, Tennessee 37831-6377

³Manne Siegbahn Laboratory at Stockholm University, S-104 05 Stockholm, Sweden

⁴FOM-Institute for Atomic and Molecular Physics, Kruislaan 407, 1098 SJ Amsterdam, The Netherlands

⁵Max-Planck-Institut für Kernphysik and Physikalisches Institut der Universität Heidelberg, D-69029 Heidelberg, Germany

⁶Department of Particle Physics, Weizmann Institute of Science, Rehovot, 76100, Israel

(Received 22 July 1996)

Asymptotic atomic-state branching ratios for the dissociative recombination of both ${}^3\text{HeD}^+$ and ${}^4\text{HeH}^+$ have been studied using the CRYRING and TSR heavy-ion storage rings. The kinetic-energy release in the recombination process was measured for incident electron energies between 0 and 15 eV. It was found that the $\text{He}(1s^2)+\text{D},\text{H}(n=2)$ channel completely dominates at zero electron energy. The branching ratios observed slightly above the threshold for the $n=3$ state of the H (D) atom indicate a rapid switchover of the final-state population to this level. At collision energies above 10 eV many channels leading to excited He atoms are found to contribute, and also a strong angular anisotropy of the dissociation products is observed. [S1050-2947(96)50412-9]

PACS number(s): 34.80.Gs, 34.80.Ht

Dissociative recombination (DR) has been known for many years to be a very fast process if the ground electronic state of the molecular ion is crossed by a neutral, doubly excited state close to the equilibrium geometry. In recent years it has become apparent that the occurrence of this crossing is in fact a sufficient but not necessary criterion for efficient recombination [1]. In the noncrossing mode of dissociation ("tunneling mode"), a single-electron radiationless transition replaces the two-electron radiationless transition that controls the crossing mode, and the DR is driven by the kinetic-energy-derivative operator. Being the simplest case of tunneling-mode recombination, HeH^+ has recently been the subject of theoretical calculations by Sarpal *et al.* [2] using the R -matrix method for ${}^4\text{HeH}^+$, and by Guberman [3] using multichannel quantum-defect theory (MQDT) for ${}^3\text{HeH}^+$. Although a qualitative agreement exists between both theories with regard to the mechanism driving the DR and to the overall size of the DR cross section, they predict different dissociation limits at near-zero electron energy. Whereas, according to the R -matrix calculation [2], recombination to the ground state of HeH ($X^2\Sigma^+$; see Fig. 1), yielding hydrogen in the ground electronic state at large internuclear distance, has the dominant cross section, the MQDT calculation [3] predicts that the $C^2\Sigma^+$ state, leading to the asymptotic state $\text{H}(n=2)$, totally dominates the recombination route. However, since the DR is driven by the nuclear kinetic-energy operator, strong influences of isotopic effects on the final-state population cannot be excluded. The present experiments try to resolve the above theoretical discrepancy by measuring the final quantum state of the fragments released in the DR of ${}^4\text{HeH}^+$ and ${}^3\text{HeD}^+$.

Ion storage rings have recently emerged as powerful tools for the study of processes involving the interaction between ions and electrons [4–6]. Experiments on HeH^+ at CRYRING [7–9], TARN II [10,11], and TSR [12] have found quite large DR cross sections in favor of the efficiency

of the tunneling mode. Results from a single-pass merged-beams experiment [13] and a flowing afterglow Langmuir probe experiment [14], on the other hand, indicate that HeH^+ recombines very slowly. Regarding the comparison with theory, the positions of the resonances in the low-energy DR cross section observed at CRYRING for ${}^3\text{HeH}^+$ [8] and ${}^4\text{HeH}^+$ [9] are not in particularly good agreement with the respective calculations [3,2,15]. This somewhat unsatisfactory situation is balanced by the good agreement concerning the overall absolute value of the DR cross section for both ${}^3\text{HeH}^+$ and ${}^4\text{HeH}^+$.

In the present work we investigated the kinetic-energy release in dissociative recombination of ${}^3\text{HeD}^+$ and ${}^4\text{HeH}^+$ for incident electron energies in the range 0–15 eV. These experiments were carried out for ${}^3\text{HeD}^+$ at the heavy-

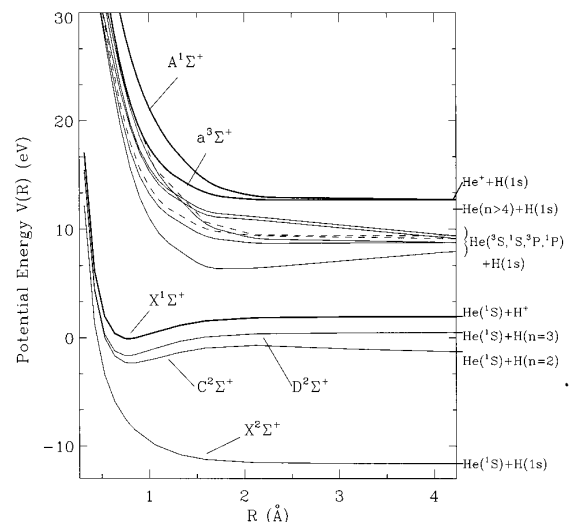


FIG. 1. Potential-energy curves of ${}^4\text{HeH}^+$ and ${}^3\text{HeD}^+$, heavy solid curves showing ionic states, thin solid curves showing ${}^2\Sigma^+$, and dashed curves ${}^2\Pi$ neutral states [3,25].

ion storage ring CRYRING, located at the Manne Siegbahn Laboratory at Stockholm University, and for ${}^4\text{HeH}^+$ at the TSR storage ring located at the Max-Planck-Institut für Kernphysik, Heidelberg. The experimental methods were similar: A molecular ion beam is stored for a period which is longer than the lifetime of the vibrational states [17]. The ion beam is then merged with a monoenergetic electron beam, which is used both for phase-space cooling of the ion beam and as an electron target. The center-of-mass energy $E_{\text{c.m.}}$ for electron-molecule collisions can be set by varying the electron-beam velocity while keeping the ion velocity fixed. The neutral fragments created in the electron cooler exit the ring after the next dipole magnet, and impinge on a detector, where they are analyzed employing an imaging technique introduced at the TSR [16].

At CRYRING, the ${}^3\text{HeD}^+$ molecules were created in an electron-impact ion source MINIS, injected into the ring at 30 keV, and further accelerated to an energy of 19.2 MeV. The collinear electron beam had a transverse electron temperature of 10 meV and an overlap region with the ion beam of 0.9 m. The beam was stored for ≈ 10 s prior to starting the measurement, which lasted for 3.5 s; the mean storage lifetime of the ions was 15 s. Dissociation products hit a two-dimensional imaging detector, located at a distance of 6.3 m from the midpoint of the electron cooler. The detector consists of three microchannel plates (MCP) with a diameter of 18 mm, and a phosphor screen. The light from the phosphor was imaged onto a free-running charge-coupled-device camera controlled by a personal computer via a fast frame grabber interface card (≈ 1400 frames per second). The frame grabber was initialized by a pulse generated at the beginning of each measurement gate. The detector was operated in a trigger mode [16] in order to suppress random coincidences between two unrelated single fragments produced by collisions with the residual gases. In this mode, the acceleration voltage between MCP and phosphor screen is switched off in $\approx 40 \mu\text{s}$ whenever an impact on the MCP is detected by a fast photomultiplier. Only frames containing hits from two fragments were analyzed, and the relative distances between these fragments were extracted. The resolution of the system is $260 \mu\text{m}$.

At the TSR, the ${}^4\text{HeH}^+$ beam was produced by a Van de Graaff accelerator with a standard Penning ion source and circulated in the TSR at a fixed energy of 1.99 MeV. The beam was merged with the electron beam of the electron cooler over a length of 1.5 m, the transverse electron temperature here being near 15 meV. The beam was electron cooled for ≈ 5 s before starting the measurement, and data were recorded for ≈ 26 s. The imaging detector used for measuring the distance between the fragments was located 6.46 m away from the center of the electron cooler and consisted of a 80-mm-diam Chevron MCP and a phosphor screen. The imaging system at the TSR worked at a rate of 25 frames per second and with a $1\text{-}\mu\text{s}$ switching time for the phosphor screen. The position resolution is $\approx 100 \mu\text{m}$. More details can be found elsewhere [16,18].

The transverse separation D (i.e., the projected distance on the surface of the detector) between two dissociation products with masses m_{H} and m_{He} at a distance L from the electron cooler depends on the kinetic-energy release (KER) $E_{k,n}$ in the center-of-mass (c.m.) frame, the initial energy of

ions (E_b), and the angle θ of the molecular axis during dissociation with respect to the electron beam, and can be expressed as $D = L\delta_n \sin\theta$ with $\delta_n = \sqrt{E_{k,n}/E_b(m_{\text{He}} + m_{\text{H}})/\sqrt{m_{\text{He}}m_{\text{H}}}}$ [16,18,19]. The excitation energy E_n of the fragments relative to the initial rovibrational state of the molecular ion is then given by energy conservation as $E_n = E_{\text{c.m.}} - E_{k,n}$. The spectrum of transverse distances, $P(D)$, is broadened by the finite ion-electron interaction length and by the angular distribution of dissociation products. Analytical expressions can be derived for various initial angular distribution and are given in Ref. [18]. The final projected distance spectrum $P(D)$ is a sum of distributions $P_n(D)$ for the energetically allowed final states with weights b_n representing the branching ratios.

By controlling the electron-ion relative velocity, transverse distance spectra were measured at various collision energies $E_{\text{c.m.}}$ with a c.m. energy spread full width at half maximum [20] ranging from the transverse electron temperature at near-zero energies up to ≈ 150 meV for $E_{\text{c.m.}} = 15$ eV. The electron and the ion beam could be aligned to each other within ≤ 1 mrad by optimizing the electron cooling process in the storage ring, so that the c.m. energies arising from beam misalignments could be kept below 1 meV. Analytical expressions of the projected distance spectrum, taking into account the finite electron-ion interaction length and angular distributions specified below, were fitted to the data. Contributions to the transverse distance spectra from different channels overlapped and could be resolved if their KER differed by $\geq 10\%$.

In Fig. 2 we show the transverse distance spectra measured at low c.m. energy for ${}^3\text{HeD}^+$ (CRYRING) and for ${}^4\text{HeH}^+$ (TSR). Different projected-distance scales apply to the two setups since the beam energies and the flight paths of DR products are different. At zero c.m. energy the only two dissociation limits energetically allowed for molecular ions in the ground vibrational level are $\text{He}(1s^2) + \text{H}(\text{D})(n=1,2)$, the corresponding KER for ${}^4\text{HeH}^+$ (${}^3\text{HeD}^+$) being 11.75 (11.74) eV and 1.55 (1.54) eV for $n=1$ and 2, respectively [21–24]. Both spectra shown in Fig. 2 were fitted assuming isotropic angular distributions of the dissociation products with the KER as a free parameter. The fits yield 1.55 eV for ${}^4\text{HeH}^+$ and 1.52 eV for ${}^3\text{HeD}^+$, indicating a final state $n=2$ for the H (D) fragments. No events corresponding to the production of ground-state H (D) atoms were found above the background level. Also, the distributions do not indicate the presence of any vibrationally or electronically excited components in the ion beam. This last point contradicts the suggestion [13] that the relatively high DR rate observed for ${}^4\text{HeH}^+$ could be due to ions in the metastable $a^3\Sigma^+$ state, for which curve crossings with doubly excited neutral states exist. In such a case, the KER would have been ≈ 0.2 eV. The present results are clearly in agreement with the theoretical calculations performed for ${}^3\text{HeH}^+$ [3] using the MQDT approach, which predict the dominant dissociative route to be the $C^2\Sigma^+$ state yielding excited $\text{H}(\text{D})(n=2)$ atoms. They are in disagreement with the R -matrix theory [2] for the DR of ${}^4\text{HeH}^+$, which predicts that the main channel near-zero electron energy should yield ground-state hydrogen atoms.

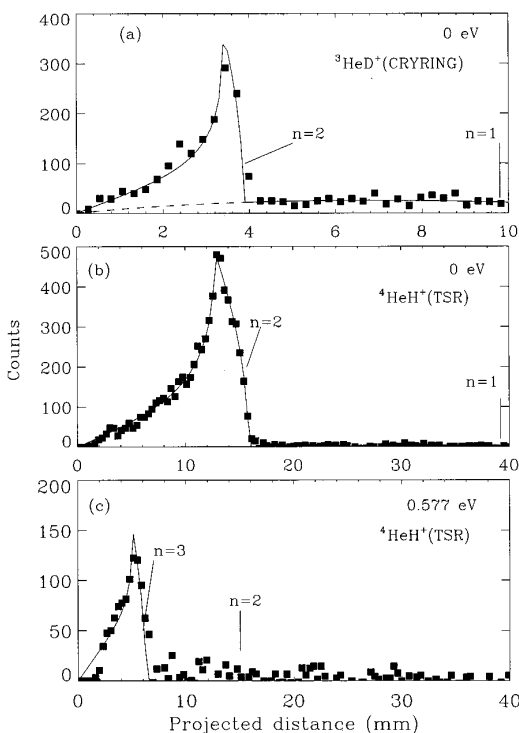


FIG. 2. Projected distance distributions for low c.m. energies: (a) ${}^3\text{HeD}^+$ at $E_{c.m.}=0$ (CRYRING); (b) ${}^4\text{HeH}^+$ at $E_{c.m.}=0$ (TSR); (c) ${}^4\text{HeH}^+$ at $E_{c.m.}=0.577$ eV (TSR). The solid lines are the fitted distributions and the dashed line in (a) is a fit to the background. Expected positions are shown in (a) and (b) for the D(H)($n=1$) fragment and in (c) for H($n=2$).

Figure 2(c) shows the projected distance distribution resulting from the DR of ${}^4\text{HeH}^+$ obtained for an electron energy $E_{c.m.}=0.577$ eV, lying 0.244 eV above the threshold for $\text{He}(1s^2)+\text{H}(n=3)$. Using the fitting procedure described above, a KER of 0.243 eV was found. No trace of the H($n=2$) state was seen above the background, which suggests that a rapid switchover in the branching ratios occurs as soon as the H($n=3$) state becomes energetically allowed. The exact reason for this drastic change is not clear, as no theoretical calculations have been performed yet for these electron energies.

Transverse distance distributions were also measured (Fig. 3) at various electron energies around the high-energy resonance of the DR cross section [7,9,10]. The spectra measured for ${}^3\text{HeD}^+$ at $E_{c.m.}=10$ and 11 eV show very similar features; the projected distance distribution at $E_{c.m.}=11$ eV is shown in Fig. 3(a). There appear two prominent peaks with very different shapes, the one at higher KER (larger distance) having a form characteristic of isotropic fragmentation, whereas the other one suggests that the molecular ions dissociate mainly parallel to the electron-beam direction [16,18,19]. At these energies, the recombination can yield several asymptotic states which (for $E_{c.m.}=10$ eV) combine a ground-state D atom with an excited ${}^3\text{He}$ atom in the configurations $1s2s$ or $1s2p$; at $E_{c.m.}=11$ eV, the ${}^3S(1s3s)$ state is also open. To fit the spectrum shown in Fig. 3(a), an anisotropy $\propto \cos^2\theta$ in the angular distribution was used for the low-KER peak, whereas the high-KER peak was fitted with an isotropic angular distribution [16,18]. At $E_{c.m.}=10$ eV, a fraction 0.52 ± 0.08 of the molecules dissociates to

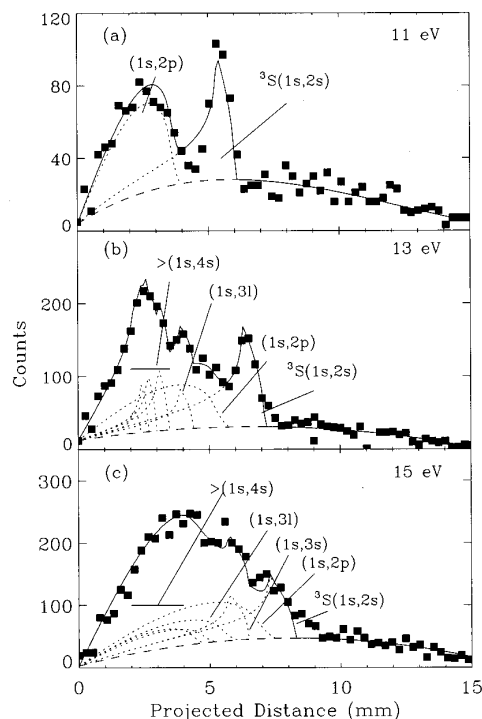


FIG. 3. Projected distance distributions for higher c.m. energies (CRYRING): (a) $E_{c.m.}=11$ eV, (b) $E_{c.m.}=13$ eV, (c) $E_{c.m.}=15$ eV. The solid lines are fits with individual contributions indicated by the broken lines and a background indicated by the dashed lines.

$\text{He}[{}^3S(1s2s)]$ and 0.48 ± 0.1 to $\text{He}(1s2p)$. At an electron energy of 11 eV, the values are left basically unchanged (0.49 ± 0.08 and 0.51 ± 0.06 , respectively). Because of the very small KER leading to the ${}^3S(1s3s)$ state (40 meV at $E_{c.m.}=11$ eV), the projected distance between the two fragments was too small to be measured with the present system. No contribution from the ${}^1S(1s2s)$ limit was found at these energies.

At higher collision energies, more excited final states become energetically allowed. The branching ratios at $E_{c.m.}=12$ eV were found to be 0.32 ± 0.05 for ${}^3S(1s2s)$, 0.40 ± 0.09 for $1s2p$, 0.10 ± 0.04 for $1s3s$, and 0.18 ± 0.04 for other He($n=3$) levels. Figure 3(b) shows the spectrum measured at a collision energy of 13 eV. The fit resulted in branching ratios of 0.33 ± 0.05 for ${}^3S(1s2s)$, 0.31 ± 0.05 for $1s2p$, 0.08 ± 0.03 for He($n=3$), 0.18 ± 0.08 for He($n=4$), and 0.10 ± 0.05 for higher limits. Since the number of free parameters makes it difficult to obtain a reliable fit, a \cos^2 -like distribution, as found for $E_{c.m.}=10$ and 11 eV, was used for dissociation into $1s2p$ also at higher $E_{c.m.}$, whereas the remaining channels were fitted assuming an isotropic fragmentation.

A strong tendency to produce highly excited ${}^3\text{He}$ atoms ($n\geq 4$) in a direction parallel to the electron beam was found at an electron energy of ≥ 15 eV [see Fig. 3(c)]. The branching ratio for these dissociation limits is 0.25 ± 0.08 . The dissociation decreases for the ${}^3S(1s2s)$ limit ($b_n=0.19\pm 0.03$) but remains still significant for the $1s2p$ limit ($b_n=0.28\pm 0.08$). The formation of $1s3s$ states occurs with a branching ratio of 0.11 ± 0.03 , and that of other He($n=3$) states with $b_n=0.17\pm 0.03$. It is important to point out that the exact functional dependence of the angular

anisotropy is difficult to extract from the two-dimensional data, so that a \cos^2 distribution should be considered as representative of an orientation effect in which the molecule dissociates preferentially along the electron-beam direction.

As discussed by Orel *et al.* [25], there are five $^2\Sigma$ states and two $^2\Pi$ states converging to the $a^3\Sigma^+$ and $A^1\Sigma^+$ ion states (see Fig. 1) that contribute to the DR cross section in this energy range. Our results are in partial agreement with the calculation of Orel *et al.*: The branching ratios measured at $E_{c.m.} \geq 10$ eV show that indeed these are the important states for the DR. However, the population distribution among these states is found to be different: Whereas the theory indicates that 100% of the recombination would lead to the He [$^3S(1s2s)$] limit through the lowest $^2\Sigma(1\sigma 2\sigma^2)$ molecular state for $E_{c.m.}$ up to 12 eV, it is found that more states are populated, and the lowest $^2\Sigma$ level does not carry more than 50% of the population. Also, at 15 eV, the He [$^3S(1s2s)$] fraction is measured to be less than 20%, while the theoretical prediction puts this branching ratio to 50%. Although the calculations were done for $^4\text{HeH}^+$, the electronic matrix elements for the direct DR should be the same, and only a small shift in the resonance shape is expected due to the difference in the vibrational wave function for the different isotopes.

Another important aspect of these measurements is the anisotropy which is observed for the angular distribution of the fragments at high electron energies. Zajfman *et al.* [16] and Amitay *et al.* [18] have observed angular anisotropies also in the DR of HD^+ and CH^+ . The exact physical reason for these effects is not clear. Although a propensity rule, given by Dunn [26] based on symmetry arguments, offers a theoretical basis for predicting angular anisotropies in electron-molecule interaction, the present results cannot be reconciled with these rules. Dunn's rules predict either isotropic or transversally peaked distributions for our case, whereas the experimental distributions are either isotropic or \cos^2 -like (i.e., longitudinally peaked). However, subsequent

theoretical developments by O'Malley and Taylor [27] have demonstrated that Dunn's rules are valid only when the lowest partial wave of the incident-electron wave function is absorbed in forming the resonant state. This assumption might be in default for HeH^+ , and detailed theoretical calculations of general angular distributions for DR fragments are thus needed.

To conclude, the branching-ratio measurement for the DR of HeH^+ with low-energy electrons is in excellent agreement with the MQDT theory [3] but in contradiction with the R -matrix theory [2]. The reason for the difference between the two theories is not clear, especially as both of them seem to be in qualitative agreement with the shape of the measured cross section and in quantitative agreement with its absolute value. The disagreement might be due to an avoided crossing between two of the dissociative curves at very short internuclear distances. Indeed, one of the ingredients of the R -matrix type of calculation is that it requires the orbitals' character to remain fixed for all internuclear distances [2]. However, detailed calculations are required in order to shed more light on this interesting discrepancy.

We are very grateful to the staff members of the Manne Siegbahn Laboratory for valuable help during the experiment at CRYRING. A special thanks we address to L. Bagge for helping in rebuilding of the beamline. For efficient assistance in the TSR experiment we thank the accelerator staff of the MPI. The CRYRING work was supported by the Swedish Natural Science Research Council and by the Göran Gustafsson Foundation; the TSR work by the German Federal Minister for Education, Science, Research and Technology (BMBF) under Contract No. 06HD562I(3). W.J.v.d.Z. acknowledges support from the Foundation for Fundamental Research on Matter (FOM) and financial support from the Netherlands Organization for Research (NWO). We gratefully acknowledge the support of this joint activity from the Human Capital and Mobility Programme of the European Community.

-
- [1] D. R. Bates, *Adv. At. Mol. Opt. Phys.* **34**, 427 (1994).
 [2] B. K. Sarpal, J. Tennyson, and L. A. Morgan, *J. Phys. B* **27**, 5943 (1994).
 [3] S. L. Guberman, *Phys. Rev. A* **49**, R4277 (1994).
 [4] G. Kilgus *et al.*, *Phys. Rev. Lett.* **64**, 737 (1990).
 [5] F. Bosch, in *The Physics of Electronic and Atomic Collisions*, edited by T. Andersen *et al.* (AIP Press, New York, 1993), p. 432.
 [6] M. Larsson, *Rep. Prog. Phys.* **58**, 1267 (1995).
 [7] G. Sundström *et al.*, *Phys. Rev. A* **50**, R2806 (1994).
 [8] J. R. Mowat *et al.*, *Phys. Rev. Lett.* **74**, 50 (1995).
 [9] C. Strömholm *et al.*, *Phys. Rev. A* **54**, 3086 (1996).
 [10] T. Tanabe *et al.*, *Phys. Rev. Lett.* **70**, 422 (1993).
 [11] T. Tanabe *et al.*, *Phys. Rev. A* **49**, R1531 (1994).
 [12] Z. Amitay *et al.* (unpublished).
 [13] F. B. Yousif *et al.*, *Phys. Rev. A* **49**, 4610 (1994).
 [14] N. G. Adams and D. Smith, in *Dissociative Recombination: Theory, Experiment and Applications*, edited by J. B. A. Mitchell and S. L. Guberman (World Scientific, Singapore, 1989), p. 124.
 [15] S. L. Guberman, in *XIXth International Conference on the Physics of Electronic and Atomic Collisions*, edited by L. J. Dubé, J. B. A. Mitchell, J. W. McConkey, and C. E. Brion (AIP, New York, 1995), p. 307.
 [16] D. Zajfman *et al.*, *Phys. Rev. Lett.* **75**, 814 (1995).
 [17] S. Datz and M. Larsson, *Phys. Scr.* **46**, 343 (1992).
 [18] Z. Amitay *et al.*, *Phys. Rev. A* **54**, 4032 (1996).
 [19] W. J. van der Zande *et al.*, *Phys. Rev. A* (to be published).
 [20] A. Wolf *et al.*, in *Dissociative Recombination: Theory, Experiment and Applications III*, edited by D. Zajfman *et al.* (World Scientific, Singapore, 1996), p. 47.
 [21] L. Wolniewicz, *J. Chem. Phys.* **43**, 1087 (1974).
 [22] W. H. Miller and H. F. Schaefer III, *J. Chem. Phys.* **53**, 1421 (1970).
 [23] K. P. Huber and G. Herzberg, *Molecular Spectra and Molecular Structure* (Van Nostrand Reinhold Co., New York, 1979), Vol. IV.
 [24] S. Bashkin and J. O. Stoner, Jr., *Atomic Energy Levels and Grotrian Diagrams* (North-Holland, Amsterdam, 1975), Vol. I.
 [25] A. E. Orel, K. C. Kulander, and T. N. Rescigno, *Phys. Rev. Lett.* **74**, 4807 (1995).
 [26] G. H. Dunn, *Phys. Rev. Lett.* **8**, 62 (1962).
 [27] T. F. O'Malley and H. S. Taylor, *Phys. Rev.* **176**, 207 (1968).